A&A, 692, L8 (2024)
https://doi.org/10.1051/0004-6361/202452049

Astronomy & Astrophysics

Letter to the Editor

Mass evolution of broad-line regions to explain the luminosity variability of broad Hα in the tidal disruption event ASASSN-14li

XueGuang Zhang[⋆]

Guangxi Key Laboratory for Relativistic Astrophysics, School of Physical Science and Technology, GuangXi University, Nanning 530004, PR China

Received 29 August 2024 / Accepted 19 November 2024

ABSTRACT

We propose an oversimplified model to explain the different variability trends in the observed broad Hα emission line luminosity, $L_{\mathrm{H}\alpha}(t)$, and the tidal disruption event (TDE) model-determined bolometric luminosity, $L_{\mathrm{bol}}(t)$, of the TDE ASASSN-14li. Assuming that broad emission line regions (BLRs) in the central accretion disk are related to materials accreted onto the central black hole of a TDE, the mass evolution of central BLRs, $M_{\mathrm{BLRs}}(t)$, can be determined as the maximum mass, $M_{\mathrm{BLRs},0}$, of central BLRs minus the corresponding accreted mass in a TDE. Meanwhile, through the simple linear dependence of broad Balmer emission line luminosity on the mass of BLRs, the mass evolution of central BLRs, $M_{\mathrm{BLRs}}(t)$, can be applied to describe the observed $L_{\mathrm{H}\alpha}(t)$. Although our proposed model is oversimplified – with only one free model parameter, $M_{\mathrm{BLRs},0}$ – with $M_{\mathrm{BLRs},0} \sim 0.02\,\mathrm{M}_{\odot}$, it describes the observed $L_{\mathrm{H}\alpha}(t)$ in the TDE ASASSN-14li well. Meanwhile, the oversimplified model also roughly describes the observed $L_{\mathrm{H}\alpha}(t)$ in the TDE ASASSN-14ae. The reasonable descriptions of the observed $L_{\mathrm{H}\alpha}(t)$ in ASASSN-14li and ASASSN-14ae indicate that our oversimplified model is probably efficient enough to describe mass evolutions of M_{BLRs} related to central accreted debris in TDEs.

Key words. galaxies: active – galaxies: nuclei – quasars: emission lines

1. Introduction

ASASSN-14li (z = 0.0206), a well-known tidal disruption event (TDE) candidate, was first detected by Holoien et al. (2016) based on its six-month multiband variability. Mockler et al. (2019) have since provided the best descriptions of the long-term multiband photometric light curves using the theoretical TDE model MOSFIT (the public code of Modular Open-Source Fitter for Transients; Guillochon & Ramirez-Ruiz 2013; Guillochon et al. 2014): a $0.2\,\mathrm{M}_{\odot}$ main-sequence star tidally disrupted by the central supermassive black hole (BH) with a mass of about $9 \times 10^{6}\,\mathrm{M}_{\odot}$. Mockler et al. (2019) provide reliable evidence that ASASSN-14li is a normal optical TDE. More recent descriptions and discussions on MOSFIT can be found in Nicholl et al. (2022). In addition to the long-term multiband photometric variability expected based on the TDE model (Holoien et al. 2016; Mockler et al. 2019), ASASSN-14li's Balmer emission line luminosity, $L_{\mathrm{H}\alpha}(t)$, also varies in the long term (Holoien et al. 2016). Study of the long-term variability of the $L_{\mathrm{H}\alpha}(t)$ in ASASSN-14li should provide valuable clues as to the evolution of broad emission line regions (BLRs) related to accreted TDE debris.

For the TDE ASASSN-14li, the time-dependent optical continuum luminosity, $L_{5100}(t)$, at rest wavelength 5100 Å can be determined based on the TDE-model-determined variability of bolometric luminosity (as well as the corresponding variability of the accretion rate) as shown in Fig. 8 of Mockler et al. (2019) by simply scaling the accepted bolometric luminosity linearly with the optical continuum luminosity, as in normal broad-line active galactic nuclei (AGNs), as discussed in Richards et al. (2006), Duras et al. (2020), Netzer (2020), and Spinoglio et al. (2024) for accreting BH systems. Meanwhile, if we accept that the physical properties of BLRs related to TDE debris are similar to those of normal BLRs in broad-line AGNs for recombination broad Balmer emission lines, using the linear dependence of the $L_{\mathrm{H}\alpha}$ for the broad Balmer emission lines from central BLRs on the optical continuum luminosity, L_{5100}, at the rest wavelength of normal quasars, 5100 Å, as shown in Greene & Ho (2005, the linear dependence can also be checked in the database of SDSS quasars in Shen et al. 2011), the variability trend of the time-dependent $L_{\mathrm{H}\alpha}(t)$ should be similar to the trend of the time-dependent bolometric luminosity, $L_{\mathrm{bol}}(t)$, of ASASSN-14li. However, as shown in Fig. 1, the trend of the time-dependent $L_{\mathrm{H}\alpha}(t)$ is very different from the trend of the time-dependent $L_{\mathrm{bol}}(t)$ for ASASSN-14li; this indicates that potential evolution properties of the central BLRs related to TDE debris should be considered, which is our main objective here.

Furthermore, for the BLRs related to accreted debris in TDEs, the entirety of the material in the BLRs is from tidally disrupted stars. By considering the evolution of central BLRs related to TDE debris, especially the mass evolution of central BLRs, to explain the $L_{\mathrm{H}\alpha}(t)$ in ASASSN-14li, we should find clues as to the mass of the central BLRs in ASASSN-14li. This manuscript is organized as follows. Section 2 presents the main hypotheses and results regarding the observed $L_{\mathrm{H}\alpha}(t)$ in ASASSN-14li using an oversimplified model that assumes that the mass evolution of central BLRs is related to TDE debris. Section 3 presents the oversimplified mass evolution model. Section 4 gives a summary of our work and our

⋆ Corresponding author; xgzhang@gxu.edu.cn

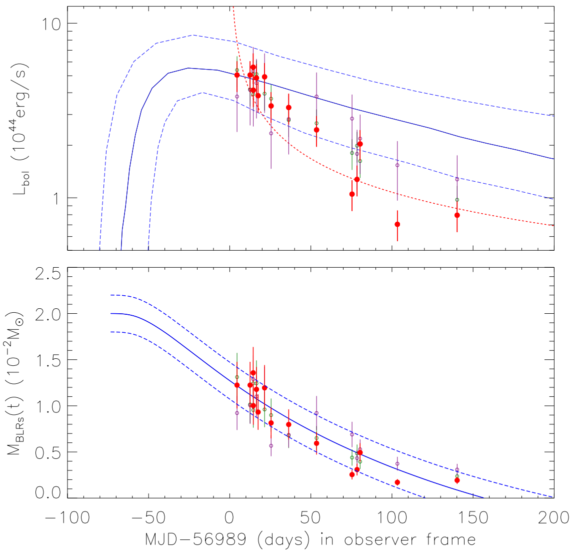

Fig. 1. Variability of $L_{\rm bol}(t)$ and $M_{\rm BLRs}(t)$ in the TDE ASASSN-14li. Top panel: MOSFIT-determined time-dependent bolometric luminosity $L_{\rm bol}(t) = \eta \dot{M}_a(t)c^2$ (solid blue line) and the corresponding confidence bands (dashed blue lines) in ASASSN-14li. Solid circles plus error bars in red show the scaled $L_{\rm H\alpha}(t) \times k_{cl}$ with $k_{cl} = 5000$, open circles plus error bars in dark green and in purple show the corresponding results with $k_{cl} = 14\,000$ and $k_{cl} = 7500$ applied to the observed $L_{\rm H\beta}(t)$ and $L_{\rm He}(t)$ in ASASSN-14li. Bottom panel: Determined $M_{\rm BLRs}(t)$ (solid blue line) applied to describe the $L_{\rm H\alpha}(t) = k_{\rm BLRs} \times M_{\rm BLRs}(t)$ in ASASSN-14li, with dashed blue lines for the determined confidence bands after accepting the uncertainties of the $M_{\rm BLRs,0}$. Solid circles plus error bars in red show the scaled $L_{\rm H\alpha}(t)/k_{\rm BLR}$ with $k_{\rm BLRs} = 8.25 \times 10^{42}$ erg/s/M$_\odot$, open circles plus error bars in dark green and in purple show the corresponding results with $k_{\rm BLRs} = 2.94 \times 10^{42}$ erg/s/M$_\odot$ and $k_{\rm BLRs} = 5.50 \times 10^{42}$ erg/s/M$_\odot$ applied to the observed $L_{\rm H\beta}(t)$ and $L_{\rm He}(t)$ in ASASSN-14li.

conclusions. We have adopted the cosmological parameters $H_0 = 70\,{\rm km \cdot s^{-1}\,Mpc^{-1}}$, $\Omega_\Lambda = 0.7$, and $\Omega_{\rm m} = 0.3$.

2. Main hypotheses and main results

The top panel of Fig. 1 shows the observed $L_{\rm H\alpha}(t)$ of ASASSN-14li, which is similar to that shown in Fig. 7 of Holoien et al. (2016). The time-dependent $L_{\rm H\alpha}(t)$ can be described as

$$L_{\rm H\alpha}(t) \propto t^{-0.638\pm0.046}. \tag{1}$$

Meanwhile, based on the reported TDE model parameters in Mockler et al. (2019), the MOSFIT version for the standard theoretical TDE model (Guillochon & Ramirez-Ruiz 2013; Guillochon et al. 2014) can be applied to determine the time-dependent bolometric luminosity, $L_{\rm bol}(t)$. It is clear that the variability trend in the observed time-dependent $L_{\rm H\alpha}(t)$ is very different from the trend in the time-dependent $L_{\rm bol}(t)$ in ASASSN-14li. Here, in order to compare the $L_{\rm bol}(t)$ with the observed $L_{\rm H\alpha}(t)$ in the top panel of Fig. 1, a scaled factor $k_{cl} = 5000$ is applied, leading the scaled $L_{\rm H\alpha}(t) \times k_{cl}$ to have similar magnitudes as $L_{\rm bol}(t)$ around MJD-56989 = 10 days. The scaled factor k_{cl} has no other special physical meaning; it is only applied so that the scaled $L_{\rm H\alpha}(t) \times k_{cl}$ is clearly seen in the top panel of Fig. 1.

Unlike for the typically steady BLRs in normal broad-line AGNs, which lead to a linear correlation between bolometric luminosity and broad-line luminosity, there should be mass evolutions of the central BLRs related to central accreted debris in TDEs. This could explain the results shown in the top panel of Fig. 1 for ASASSN-14li. Based on this, we propose the following three hypotheses.

First, the upper limit of the total mass of central BLRs, $M_{\rm BLRs}$, related to TDE debris is the total accreted mass of the TDEs. For ASASSN-14li, the total accreted mass is about 40% of the mass of the tidally disrupted main-sequence star, which has a stellar mass of 0.2 M$_\odot$ as reported in Mockler et al. (2019), leading the upper limit of $M_{\rm BLRs}$ to be about 0.08 M$_\odot$. Since there are no other sources of broad Balmer emission line material in TDEs, especially TDEs in quiescent galaxies like ASASSN-14li, this hypothesis is reasonable.

Second, the broad Balmer emission line luminosity scales with the mass of central BLRs, $M_{\rm BLRs}$, related to TDE debris. As discussed in the classic textbook Astrophysics of Gaseous Nebulae and Active Galactic Nuclei (Osterbrock & Ferland 2006), the broad Balmer emission line (here, broad Hα) luminosity from the BLRs can be described as

$$\begin{aligned} L_{\rm H\alpha} &= n_e \times n_p \times \alpha^{\rm eff}_{\rm H\alpha} \times h \times \nu_{\rm H\alpha} \times V_{\rm BLRs} \times \epsilon \\ M_{\rm BLRs} &\sim n_p \times M_H \times V_{\rm BLRs} \times \epsilon \\ L_{\rm H\alpha} &= \frac{1}{M_H} \times n_e \times \alpha^{\rm eff}_{\rm H\alpha} \times h \times \nu_{\rm H\alpha} \times M_{\rm BLRs} \\ &= k_{\rm BLRs} \times M_{\rm BLRs}, \end{aligned} \tag{2}$$

with n_e and n_p the electron and proton density, $\alpha^{\rm eff}_{\rm H\alpha}$ the effective recombination coefficient of the Hα emission line, h the Planck constant, $\nu_{\rm H\alpha}$ the emission frequency of Hα, M_H the proton mass, $V_{\rm BLRs}$ the total volume of the BLRs, and ϵ the filling factor of the material in the BLRs. If we assume a constant n_e and $\alpha^{\rm eff}_{\rm H\alpha}$ in the BLRs related to TDE debris, the variability of the broad Balmer emission line luminosity simply depends on the time-dependent $M_{\rm BLRs}(t)$ (the mass evolution of central BLRs). As discussed in Guillochon et al. (2014), the electron density, n_e, decreases with radius, r, more slowly than r^{-4} in physical environments around TDEs; therefore, a constant n_e is a reasonable assumption. Further discussion on a few effects of a temperature-dependent $\alpha^{\rm eff}_{\rm H\alpha}$ can be found in the following section. One point should be noted. As shown in the first sub-equation above, the parameters of n_e and $\alpha^{\rm eff}_{\rm H\alpha}$ are coupled. Therefore, we did not set individual values for the parameters but instead selected the $k_{\rm BLRs}$ parameter to represent the product of these parameters.

Third, assuming the central BLRs is located in the central accretion disk (the BLRs are part of the central accretion disk), the BH accreting mass should lead to a decrement of the BLR mass, $M_{\rm BLRs}$. In other words, the accreting process leads $M_{\rm BLRs}(t)$ to decrease over time, which can be described as

$$M_{\rm BLRs}(t) = M_{\rm BLRs,0} - \int_{t' \le t} \dot{M}_a(t'){\rm d}t', \tag{3}$$

with $\dot{M}_a(t)$ the physical accretion rates of TDEs and $M_{\rm BLRs,0}$ the maximum mass of central BLRs prior to mass loss. Due to the bolometric luminosity $L_{\rm bol}(t) = \eta \times \dot{M}_a(t)c^2$ (η is the energy transfer efficiency, c the speed of light), the $L_{\rm bol}(t)$ shown in the top panel of Fig. 1 also can be accepted as the variability pattern of the $\dot{M}_a(t)$ in ASASSN-14li with the MOSFIT-determined η = 20%. For ASASSN-14li, the $L_{\rm bol}(t)$ (the corresponding $\dot{M}_a(t)$) was determined using MOSFIT by Mockler et al. (2019). Mainly due to both its high-quality $L_{\rm H\alpha}(t)$ and the well-determined TDE-model-expected $L_{\rm bol}(t)$ (or TDE-model-expected $\dot{M}_a(t)$) reported in the literature, we chose ASASSN-14li as the subject of our study. Moreover, disk-like BLRs related to TDE debris (or BLRs related to TDE debris in central accretion disks in

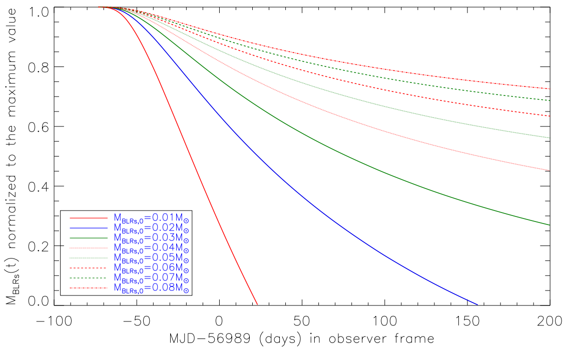

Fig. 2. Effects of $M_{\rm BLRs,0}$ on $M_{\rm BLRs}(t)$. To show clear comparisons, each $M_{\rm BLRs}(t)$ has been normalized to its maximum value. Different line styles in different colors represent the results for different $M_{\rm BLRs,0}$ values, as shown in the legend in bottom-left corner. The solid blue line shows the same $M_{\rm BLRs}(t)$ as that shown in the bottom panel of Fig. 1.

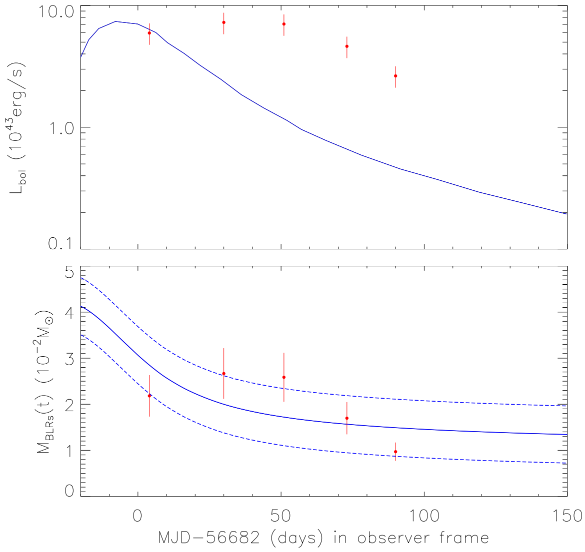

Fig. 3. Same as Fig. 1, but for ASASSN-14ae.

TDEs) have been reported for some optical TDE candidates with double-peaked (or very asymmetric) broad Balmer emission lines, including SDSS J0159 (Zhang 2021), ASASSN-14ae (Holoien et al. 2014), PTF09djl (Liu et al. 2017), ASASSN-14li (Cao et al. 2018), PS18kh (Holoien et al. 2019), AT2018hyz (Short et al. 2020; Hung et al. 2020), AT2020zso (Wevers et al. 2022), AT2019qiz (Short et al. 2023), and SDSS J1605 (Zhang 2024a). Therefore, this third hypothesis, that BLRs are located in central accretion disks in TDEs, is also reasonable.

Based on these three simple hypotheses, the observed time-dependent broad Balmer emission line luminosity $L_{\rm H\alpha}(t) = k_{\rm BLRs} \times M_{\rm BLRs}(t)$ can be determined from the time-dependent $M_{\rm BLRs}(t)$ with only one free model parameter, $M_{\rm BLRs,0}$. Based on the Levenberg-Marquardt least-squares minimization technique (Markwardt 2009), we determined the best descriptions of the $L_{\rm H\alpha}(t)$ linearly scaled with $M_{\rm BLRs}(t)$ using the determined $M_{\rm BLRs,0} = 0.02 \pm 0.002\,{\rm M}_\odot$ (about 25% of the total accreted mass) and $k_{\rm BLRs} \sim 8.25\times10^{42}\,{\rm erg/s/M}_\odot$ for ASASSN-14li; they are shown in the bottom panel of Fig. 1.

Therefore, the oversimplified model with only one free model parameter, $M_{\rm BLRs,0}$ (the factor $k_{\rm BLRs}$ was only used to convert the $L_{\rm H\alpha}(t)$ in units of erg/s to $M_{\rm BLRs}(t)$ in units of ${\rm M}_\odot$) can be applied to describe the observed $L_{\rm H\alpha}(t)$ in ASASSN-14li. Meanwhile, considering the linear correlations between $L_{\rm H\alpha}(t)$ and $L_{\rm H\beta}(t)$, where $L_{\rm H\beta}(t)$ is the broad Hβ line luminosity, and between $L_{\rm H\alpha}(t)$ and $L_{\rm He}(t)$, where $L_{\rm He}(t)$ is the broad He II line luminosity (as shown in Holoien et al. 2016), the corresponding results for $L_{\rm H\beta}(t)$[1] and $L_{\rm He}(t)$ in ASASSN-14li can be obtained from the accepted $k_{cl} = 14\,000$ and $k_{\rm BLRs} = 2.94\times10^{42}\,{\rm erg/s/M}_\odot$ and the accepted $k_{cl} = 7500$ and $k_{\rm BLRs} = 5.5 \times 10^{42}\,{\rm erg/s/M}_\odot$, respectively, as shown in Fig. 1.

3. Discussion

First we discuss the effects of different $M_{\rm BLRs,0}$. Some $M_{\rm BLRs}(t)$ values are shown in Fig. 2 as a function of different values of $M_{\rm BLRs,0}/{\rm M}_\odot$, from 0.01 to 0.08 (the total accreted mass in ASASSN-14li). It is clear that different values of $M_{\rm BLRs,0}$ can lead to different $M_{\rm BLRs}(t)$ over time. Moreover, the results shown in Fig. 2 also indicate that there should be different variability trends of broad Balmer emission line luminosity over time in different TDE candidates, such as a higher $M_{\rm BLRs,0}$ related to the total accreted mass leading to a much flatter time-dependent $L_{\rm H\alpha}(t)$.

Second, it is necessary to check whether the factor $k_{\rm BLRs} = 8.25 \times 10^{42}\,{\rm erg/s/M}_\odot$ is reasonable for ASASSN-14li. As discussed in Osterbrock & Ferland (2006), the total ionized mass of BLRs in common Seyfert galaxies should be about $40\,{\rm M}_\odot$ for $L_{\rm H\alpha,Book} \sim 10^{43}\,{\rm erg/s}$ with $n_e \sim 10^9\,{\rm cm}^{-3}$. For ASASSN-14li, the maximum $L_{\rm H\alpha,0} \sim 10^{41}\,{\rm erg/s}$ leads the estimated $M_{\rm BLRs,0}$ to be about $40\,{\rm M}_\odot \frac{L_{\rm H\alpha,0}}{L_{\rm H\alpha,Book}} \sim 0.04\,{\rm M}_\odot$ (assuming $n_e \sim 10^9\,{\rm cm}^{-3}$), very consistent with the determined $M_{\rm BLRs,0}$ of $0.02\,{\rm M}_\odot$ in ASASSN-14li. Therefore, the applied factor $k_{\rm BLRs}$ is reasonable.

Third, it is necessary to check whether the oversimplified model can be applied to explain the variability in broad Balmer emission lines in any other TDE candidates. Along with more than 150 reported TDE candidates (e.g., those reported in Gezari et al. 2006; Cenko et al. 2012; Wyrzykowski et al. 2017; Wang et al. 2018; Gezari 2021; Sazonov et al. 2021; van Velzen et al. 2021; Zhang et al. 2022; Zhang 2022, 2024b; Yao et al. 2023, etc.), ASASSN-14ae has a broad Hα luminosity (as reported in Holoien et al. 2014), although it only has five $L_{\rm H\alpha}(t)$ data points. The MOSFIT-determined $L_{\rm bol}(t)$ from Mockler et al. (2019) and the observed $L_{\rm H\alpha}(t)$ from Holoien et al. (2014) for ASASSN-14ae are shown in the top panel of Fig. 3. The variability trend of the observed $L_{\rm H\alpha}(t)$ is very different from the trend of the MOSFIT-determined $L_{\rm bol}(t)$ for ASASSN-14ae. Our oversimplified model can thus be applied to describe the $L_{\rm H\alpha}(t)$ in ASASSN-14ae, as shown in the bottom panel of Fig. 3 with $M_{\rm BLRs,0} = 0.04 \pm 0.004\,{\rm M}_\odot$ (the MOSFIT-determined total accreted mass is about $0.04 \pm 0.01\,{\rm M}_\odot$). Similar to the expected results shown in Fig. 2, the $L_{\rm H\alpha}(t)$ being flatter than $L_{\rm bol}(t)$ leads the determined $M_{\rm BLRs,0}$ to be close to the total accreted mass in ASASSN-14ae. Here we should note that since there are only five $L_{\rm H\alpha}(t)$ data points for ASASSN-14ae, it is hard to definitively conclude that the oversimplified model describes the observed $L_{\rm H\alpha}(t)$ well. However, considering that almost all five data points lie within the confidence bands as shown in bottom panel of Fig. 3, we can conclude that the descriptions determined by our oversimplified model are roughly appropriate for ASASSN-14ae.

[1] There is a data point at MJD = 57 006 with a broad Hα to broad Hβ luminosity ratio of 1.36 (much smaller than the common values 2.8 or 3.1). Therefore, the data point at MJD=57 006 has been removed from the plot of the $L_{\rm H\beta}(t)$.

Fourth, the oversimplified model does not take the effects of the temperature-dependent effective recombination coefficient, $\alpha^{\rm eff}_{\rm H\alpha}(T)$, into account. Taking the MOSFIT-determined time-dependent photosphere temperature, $T(t)$, as shown in Fig. 8 in Mockler et al. (2019), the environment temperature can be changed from 6.76×10^4 K at MJD-56989 = 10 days to 1.08×10^5 K at MJD-56989 = 145 days for ASASSN-14li, leading to only 25% changes in $\alpha^{\rm eff}_{\rm H\alpha}(T)$. In other words, the variability of the environment temperatures leads to changes of only 25% in the observed $L_{\rm H\alpha}(t)$ for ASASSN-14li. Compared with the $L_{\rm H\alpha}$ uncertainty of about 20% and the ratio of the $L_{\rm H\alpha}(t)$ at MJD-56989 = 10 days to the $L_{\rm H\alpha}(t)$ at MJD-56989 = 145 days of 8, the effects of $\alpha^{\rm eff}_{\rm H\alpha}(T)$ can be ignored in this case. Meanwhile, based on the MOSFIT-determined results for ASASSN-14ae, the environment temperature can be changed from 1.80×10^4 K at MJD-56682 = 4 days to 2.15×10^4 K at MJD-56682 = 90 days, resulting in changes of only 9% in $\alpha^{\rm eff}_{\rm H\alpha}(T)$. Compared with the ratio of about 2 of the $L_{\rm H\alpha}(t)$ at MJD-56682 = 4 days to the $L_{\rm H\alpha}(t)$ at MJD-56682 = 90 days for ASASSN-14ae, the effects of $\alpha^{\rm eff}_{\rm H\alpha}(T)$ can also be ignored for ASASSN-14ae.

We note that there are many TDE candidates with $L_{\rm H\alpha}(t)$ values reported in the literature, such as the small sample of TDEs discussed in Charalampopoulos et al. (2022). However, we mainly considered TDEs for which the TDE-model-predicted $\dot{M}_a(t)$ (or the corresponding $L_{\rm bol}(t)$) has been determined and reported in the literature (see Eq. (3)). Determining $\dot{M}_a(t)$ through applications of the TDE model to describe long-term photometric variability is beyond the scope of this study. Therefore, only ASASSN-14li and ASASSN-14ae are discussed since their $L_{\rm bol}(t)$ (= $\eta \dot{M}_a(t) c^2$) values have been reported in Mockler et al. (2019). For the TDE candidates reported in Charalampopoulos et al. (2022) and the references therein, there are $L_{\rm H\alpha}(t)$ values but no clear information regarding TDE-model-determined $L_{\rm bol}(t)$ (or $\dot{M}_a(t)$) values. Therefore, we did not examine the TDE candidates discussed in Charalampopoulos et al. (2022).

Although our model is oversimplified and has only one free parameter, $M_{\rm BLRs,0}$, it can describe the observed time-dependent luminosity variability of broad Balmer emission lines from central BLRs related to TDE debris in ASASSN-14li and ASASSN-14ae, indicating it is efficient enough to some extent. Testing the oversimplified model with more TDEs should provide further evidence for or against its reliability. In our oversimplified model, there are no time delays between formations of BLRs and formations of central accretion disks related to TDE debris. If there is clear evidence of such times delays (t_d) between TDE-model-determined $L_{\rm bol}(t)$ and high-quality observed $L_{\rm H\alpha}(t)$ values for any TDE candidate, the $M_{\rm BLRs}(t)$ could be probably improved to

$$M_{\rm BLRs}(t) = M_{\rm BLRs,0} - \int_{t' \leq t+t_d} \dot{M}_a(t')\mathrm{d}t', \tag{4}$$

which would lead to more flexible results for expected $L_{\rm bol}(t)$ in TDEs. Unfortunately, we currently do not have any evidence of such delays.

4. Summary and conclusions

Our main conclusions are as follows.

- Based on the TDE-model-determined time-dependent bolometric luminosity, $L_{\rm bol}(t)$, and the observed time-dependent broad Hα emission line luminosity, $L_{\rm H\alpha}(t)$, of ASASSN-14li, there are no consistent variability trends in the $L_{\rm bol}(t)$ or the $L_{\rm H\alpha}(t)$. This indicates that the BLRs properties of TDE debris are different from those of the steady BLRs in normal broad-line AGNs.
- We propose an oversimplified model to explain the observed $L_{\rm H\alpha}(t)$ in ASASSN-14li after considering the BLRs related to TDE debris accreted by central BHs, which leads to a decrement of the mass of the BLRs, $M_{\rm BLRs}(t)$, over time. As such, the observed $L_{\rm H\alpha}(t)$ scales linearly with the $k_{\rm BLRs} \times M_{\rm BLRs}(t)$.
- Based on the oversimplified model with only one free model parameter, $M_{\rm BLRs,0}$ (the expected maximum mass of BLRs prior to mass loss), the observed $L_{\rm H\alpha}(t)$ in ASASSN-14li can be described with the determined parameter $M_{\rm BLRs,0} \sim 0.02 \pm 0.002\,{\rm M_\odot}$.
- The oversimplified model also roughly describes the observed $L_{\rm H\alpha}(t)$ in ASASSN-14ae.
- In future studies, different values of $M_{\rm BLRs,0}$ should be considered in the oversimplified model, along with probable time delays between formations of BLRs and formations of accretion disks. By doing so, we should obtain more flexible results for the $L_{\rm H\alpha}(t)$ in TDEs.

Acknowledgements. Zhang gratefully acknowledge the anonymous referee for giving us constructive comments and suggestions to greatly improve the paper. Zhang gratefully thanks the kind financial support from GuangXi University and the kind grant support from NSFC-12173020 and NSFC-12373014. This manuscript has made use of the public TDEFIT (https://github.com/guillochon/tdefit), MOSFIT (https://github.com/guillochon/mosfit), and the MPFIT package (http://cow.physics.wisc.edu/~craigm/idl/idl.html).

References

Cao, R., Liu, F. K., Zhou, Z. Q., Komossa, S., & Ho, L. C. 2018, MNRAS, 480, 2929
Cenko, S. B., Krimm, H. A., Horesh, A., et al. 2012, ApJ, 753, 77
Charalampopoulos, P., Leloudas, G., Malesani, D. B., et al. 2022, A&A, 659, A34
Duras, F., Bongiorno, A., Ricci, F., et al. 2020, A&A, 636, A73
Gezari, S. 2021, ARA&A, 59, 21
Gezari, S., Martin, D. C., Milliard, B., et al. 2006, ApJ, 653, L25
Greene, J. E., & Ho, L. C. 2005, ApJ, 630, 122
Guillochon, J., & Ramirez-Ruiz, E. 2013, ApJ, 767, 25
Guillochon, J., Manukian, H., & Ramirez-Ruiz, E. 2014, ApJ, 783, 23
Holoien, T. W.-S., Prieto, J. L., Bersier, D., et al. 2014, MNRAS, 445, 3263
Holoien, T. W.-S., Kochanek, C. S., Prieto, J. L., et al. 2016, MNRAS, 455, 2918
Holoien, T. W. S., Huber, M. E., Shappee, B. J., et al. 2019, ApJ, 880, 120
Hung, T., Foley, R. J., Ramirez-Ruiz, E., et al. 2020, ApJ, 903, 31
Liu, F. K., Zhou, Z. Q., Cao, R., Ho, L. C., & Komossa, S. 2017, MNRAS, 472, L99
Markwardt, C. B. 2009, ASP Conf. Ser., 411, 251
Mockler, B., Guillochon, J., & Ramirez-Ruiz, E. 2019, ApJ, 872, 151
Netzer, H. 2020, MNRAS, 488, 5185
Nicholl, M., Lanning, D., Ramsden, P., et al. 2022, MNRAS, 515, 5604
Osterbrock, D. E., & Ferland, G. F. 2006, Astrophysics of Gaseous Nebulae and Active Galactic Nuclei, 2nd edn. (Sausalito, CA: University Science Books), Chapter 13
Richards, G. T., Lacy, M., Storrie-Lombardi, L. J., et al. 2006, ApJS, 166, 470
Sazonov, S., Gilfanov, M., Medvedev, P., et al. 2021, MNRAS, 508, 3820
Shen, Y., Richards, G. T., Strauss, M. A., et al. 2011, ApJS, 194, 45
Short, P., Nicholl, M., Lawrence, A., Gomez, S., et al. 2020, MNRAS, 498, 4119
Short, P., Lawrence, A., Nicholl, M., et al. 2023, MNRAS, 525, 1568
Spinoglio, L., Fernandez-Ontiveros, J. A., & Malkan, M. A. 2024, ApJ, 964, 117
van Velzen, S., Gezari, S., Hammerstein, E., et al. 2021, ApJ, 908, 4
Wang, T., Yan, L., Dou, L., et al. 2018, MNRAS, 477, 2943
Wevers, T., Nicholl, M., Guolo, M., et al. 2022, A&A, 666, A6
Wyrzykowski, L., Zielinski, M., Kostrzewa-Rutkowska, Z., et al. 2017, MNRAS, 465, L114
Yao, Y., Ravi, V., Gezari, S., et al. 2023, ApJ, 955, L6
Zhang, X. G. 2021, MNRAS, 500, L57
Zhang, X. G. 2022, MNRAS, 516, L66
Zhang, X. G. 2024a, MNRAS, 529, L169
Zhang, X. G. 2024b, MNRAS, accepted [arXiv:2407.20616]
Zhang, W. J., Shu, X. W., Sheng, Z. F., et al. 2022, A&A, 660, A119